Syntheses, Structures, and Reactivity of Low Spin Iron(III) Complexes Containing a Single Carboxamido Nitrogen in a [FeN_5L] Chromophore

John M. Rowland, Marilyn Olmstead, and Pradip K. Mascharak*

Department of Chemistry and Biochemistry, University of California, Santa Cruz, California 95064, and the Department of Chemistry, University of California, Davis, California 95616

Received October 12, 2000

A new pentacoordinate ligand based on TPA (tris-(2-pyridylmethyl)amine), namely, *N*,*N*-bis(2-pyridylmethyl)-amine-*N*-ethyl-2-pyridine-2-carboxamide ($PaPy_3H$), has been synthesized. The iron(III) complexes of this ligand, namely, $[Fe(PaPy_3)(CH_3CN)](ClO_4)_2$ (**1**), $[Fe(PaPy_3)(Cl)]ClO_4$ (**2**), $[Fe(PaPy_3)(CN)]ClO_4$ (**3**), and $[Fe(PaPy_3)(N_3)]ClO_4$ (**4**), have been isolated and complexes **1**−**3** have been structurally characterized. These complexes are the first examples of monomeric iron(III) complexes with one carboxamido nitrogen in the first coordination sphere. All four complexes are low spin and exhibit rhombic EPR signals around $g = 2$. The solvent bound species $[Fe(PaPy_3)(CH_3CN)](ClO_4)_2$ reacts with H_2O_2 in acetonitrile at low temperature to afford $[Fe(PaPy_3)(OOH)]^+$ ($g = 2.24, 2.14, 1.96$). When cyclohexene is allowed to react with **1**/H_2O_2 at room temperature, a significant amount of cyclohexene oxide is produced along with the allylic oxidation products. Analysis of the oxidation products indicates that the allylic oxidation products arise from a radical-driven autoxidation process while the epoxidation is carried out by a distinctly different oxidant. No epoxidation of cyclohexene is observed with **1**/TBHP.

Introduction

Mononuclear non-heme iron centers have been of interest in relation to the various O_2-activating enzymes.[1−3] Examples of O_2-activating non-heme iron centers include those found in the active sites of enzymes such as lipoxygenase, α-keto acid-dependent enzymes, isopenicillin N synthase, catechol dioxygenase and in the DNA cleavage chemistry of the antitumor drug bleomycin.[4] A common characteristic of this particular subclass of iron centers is the occurrence of iron(III)-peroxo intermediates in their reaction pathways.[5−7] Recently there has been considerable effort toward development of model complexes to investigate the reactivity of mononuclear iron(III)-peroxo species.[8−21] A close scrutiny of the literature suggests that many of these mononuclear iron complexes have been derived from N-based ligands and in particular ligands of the tris-(2-pyridylmethyl)amine (TPA) type (Figure 1).[13,15,17,20,22]

These ligands afford primarily mononuclear iron(II) complexes. In contrast, the iron(III) complexes of these ligands are often oxo-bridged dinuclear species, although additional anionic ligands can stabilize the iron(III) center in mononuclear ones.[23−28] In our studies on O_2-activation by iron complexes,

(1) Que, L., Jr.; Ho, R. Y. N. *Chem. Rev*. **1996**, *96*, 2607.
(2) Feig, A. L.; Lippard, S. J. *Chem. Rev.* **1994**, *94*, 795.
(3) Wallar, B. J.; Lipscomb, J. D. *Chem. Rev*. **1996**, *96*, 2625.
(4) Nivorozhkin, A. L.; Girerd, J.-J. *Angew. Chem., Int. Ed. Engl*. **1996**, *35*, 609.
(5) Fontecave, M.; Ménage, S.; Duboc-Toia, C. *Coord. Chem. Rev*. **1998**, *178*−*180*, 1555.
(6) Mononuclear iron(III)-peroxo complexes have also been implicated in the chemistry of cytochrome P-450. See: Sono, M.; Roach, M. P.; Coulter, E. D.; Dawson, J. H. *Chem. Rev*. **1996**, *96*, 2841 and references therein.
(7) Stubbe, J.; Kozarich, J. W. *Chem. Rev*. **1987**, *87*, 1107.
(8) Guajardo, R. J.; Hudson, S. E.; Brown, S. J.; Mascharak, P. K. *J. Am. Chem. Soc.* **1993**, *115*, 7971.
(9) Nguyen, C.; Guajardo, R. J.; Mascharak, P. K. *Inorg. Chem*. **1996**, *35*, 6273.
(10) Roelfs, G.; Lubben, M.; Chen, K.; Ho, R. Y. N.; Meetsma, A.; Genseberger, S.; Hermant, R. M.; Hage, R.; Mandal, S. K.; Young, V. G.; Zang, Y.; Kooijman, H.; Spek, A. L.; Que, L., Jr.; Feringa, B. L. *Inorg. Chem*. **1999**, *38*, 1929.
(11) Roelfs, G.; Lubben, M.; Leppard, S. W.; Schudde, E. P.; Hermant, R. M.; Hage, R.; Wilkinson, E. C.; Que, L., Jr.; Feringa, B. C. *J. Mol. Catal. A.* **1997**, *117*, 223.
(12) Ho, R. Y. N.; Roelfes, G.; Feringa, B. L.; Que, L., Jr. *J. Am. Chem. Soc*. **1999**, *121*, 264.
(13) Lubben, M. Meetsma, A.; Wilkinson, E. C.; Feringa, B.; Que, L., Jr. *Angew. Chem., Int. Ed. Engl*. **1995**, *34*, 1512.
(14) Zang, Y.; Elgren, T. E.; Dong, Y.; Que, L., Jr. *J. Am. Chem. Soc*. **1993**, *115*, 811.
(15) Kim, C.; Chen, K.; Kim, J.; Que, L., Jr. *J. Am. Chem. Soc*. **1997**, *119*, 5964.
(16) Zang, Y.; Kim, J.; Dong, Y.; Wilkinson, E. C.; Appelman, E. H.; Que, L., Jr. *J. Am. Chem. Soc*. **1997**, *119*, 4197.
(17) Wada, A.; Ogo, S.; Watanabe, Y.; Mukai, M.; Kitagawa, T.; Jitsukawa, K.; Masuda, H.; Einaga, H. *Inorg. Chem*. **1999**, *38*, 3592.
(18) Ito, S.; Suzuki, M.; Kobayashi, T.; Itoh, H.; Harada, A.; Ohba, S.; Nishida, Y. *J. Chem. Soc., Dalton Trans*. **1996**, 2579.
(19) Bernal, I.; Jensen, I. M.; Jensen, K. B.; McKenzie, C. J.; Toftlund, H.; Tuchagues, J.-P. *J. Chem. Soc. Dalton Trans*. **1995**, 3667.
(20) Mialane, P.; Nivorojkine, A.; Pratviel, G.; Azéma, L.; Slany, M.; Godde, F.; Simaan, A.; Banse, F.; Kargar-Grisel, T.; Bouchoux, G.; Sainton, J.; Horner, O.; Guilhem, J.; Tchertanova, L.; Meunier, B.; Girerd, J.-J. *Inorg. Chem*. **1999**, *38*, 1085.
(21) de Vries, M. E.; La Crois, R. M. L.; Roelfes, G.; Kooijman, H.; Spek, A. L.; Hage, R.; Feringa, B. L. *Chem. Commun*. **1997**, 1549.
(22) Abbreviations used: N4Py = *N*-bis(2-pyridylmethyl)-*N*,*N*-bis(2-pyridylmethyl)amine, bppa = bis(6-pivalamido-2-pyridylmethyl)(2-pyridylmethyl)amine, tpmen = *N*-methyl-*N*,*N*′,*N*′-tris(2-pyridylmethyl)ethane-1,2-diamine, Py5 = 2,6-bis[methoxybis(2-pyridyl)methyl]pyridine.
(23) Kojima. T.; Leising, R. A.; Yan, S.; Que, L., Jr. *J. Am. Chem. Soc*. **1993**, *115*, 11328.
(24) Norman, R. E.; Holz, R. C.; Menage, S.; O'Connor, C. J.; Zhang, J. H.; Que, L., Jr. *Inorg. Chem*. **1990**, *29*, 4629.
(25) Jang, H. G.; Cox, D. D.; Que, L., Jr. *J. Am. Chem. Soc*. **1991**, *113*, 9200.
(26) Nivorozhkin, A. L.; Anxolabéhère-Mallart, E.; Mialane, P.; Davydov, R.; Guilhem, JCesario, M.; Audière, J.-P.; Girerd, J.-J.; Styring, S.; Schussler, L.; Seris, J.-L. *Inorg. Chem*. **1997**, *36*, 846.
(27) Nishida, Y.; Okuno, T.; to, S.; Harada, A.; Ohba, S.; Matsushima, H.; Tokii, T. *Chem. Lett*. **1995**, 885.

10.1021/ic001127s CCC: $20.00
Published on Web 05/10/2001

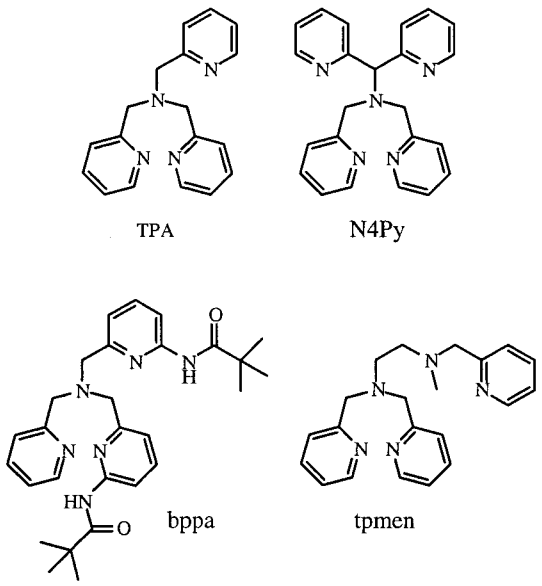

Figure 1. TPA and TPA type ligands.

we have focused mainly on mononuclear iron(III) centers.[8,9] The search for stable mononuclear iron(III) complexes led us and others to the finding that deprotonated carboxamido nitrogen is an excellent donor for iron(III) and the majority of such complexes are mononuclear.[29−35] The prevalent formation of oxo- or hydroxo-bridged polymeric species is noticeably rare in this chemistry. With this in mind, we have now designed a new pentadentate ligand based on TPA but with a built-in single carboxamide group. This ligand, namely, *N*,*N*-bis(2-pyridylmethyl)amine-*N*-ethyl-2-pyridine-2-carboxamide, is abbreviated as $PaPy_3H$ (H is the dissociable carboxamido H atom).

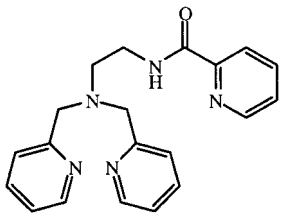

$PaPy_3H$

In this paper, we report the syntheses and structures of the parent iron(III) complex $[Fe(PaPy_3)(CH_3CN)](ClO_4)_2$ (**1**) along with two adducts $[Fe(PaPy_3)(Cl)]ClO_4$ (**2**) and $[Fe(PaPy_3)(CN)]ClO_4$ (**3**). The spectroscopic and redox properties of these species and one additional adduct $[Fe(PaPy_3)(N_3)]ClO_4$ (**4**) are also included. Complexes **1**−**3** comprise the first structurally characterized examples of iron(III) centers ligated to *one* carboxamido nitrogen.

Successful isolation of complex **1** with a labile site has allowed us to explore the reactivity of the iron(III) center with peroxides. To date, various groups have characterized mononuclear peroxo-iron(III) species by spectroscopic methods. These species have been obtained from iron complexes of ligands designed specifically to stabilize the peroxo-iron(III) unit.[10,17,19−21] In most cases, the peroxo-iron(III) species have been generated by the addition of H_2O_2 or ROOH to iron(II) complexes. The consensus is that the iron(II) center is first oxidized to iron(III) and further steps lead to the formation of the [LFe(OOR)] or [LFe(OOH)] species. This stepwise formation of peroxo-iron(III) species is supported by the recent isolation of $[(N4Py)Fe(OMe)]^{2+}$ by the addition of half an equivalent of H_2O_2 to the iron(II) starting complex. Subsequent addition of H_2O_2 yields [(N4Py)Fe(OOH)] via a simple ligand exchange.[10] In recent years, [L_nFe(OOR)] species have also been generated in solution from (μ-oxo)diiron complexes.[36−38] In addition, Wada et al. have reported the isolation of a seven coordinate peroxo-iron(III) complex that is generated by ligand exchange of a coordinated *tert*-butyl acetate ligand at an iron(III) center by *tert*-butyl hydroperoxide (TBHP).[17] It has become apparent from the latter studies that the direct addition of ROOH to iron(III) centers could be a viable reaction pathway to [LFe(OOR)] species. We were therefore interested in designing a ligand that could stabilize a mononuclear [LFe^{III}(solv)] species and eventually provide [LFe(OO^{t}Bu)] and [LFe(OOH)] via exchange of the solvent molecule by ROO^- (R = ^{t}Bu, H). In this account we report that both $[Fe(PaPy_3)(OO^tBu)]^+$ and $[Fe(PaPy_3)(OOH)]^+$ are readily formed in reactions of **1** with TBHP and H_2O_2 respectively. The former species promote alkane oxidation at room temperature while the latter is very effective in epoxidation of olefins.

Experimental Section

2-Aminomethylpyridine, *N*-Bromoethylphthalimide, picolinic acid, hydrazine monohydrate, cyclohexanol, cyclohexanone, 2-cyclohexenol, 2-cyclohexenone, iodocyclohexane and 3-bromocyclohexene, TBHP (70%), and hydrogen peroxide (30%), were obtained from Aldrich Chemical Co and used without further purification. $[Fe(DMF)_6](ClO_4)_3$ and (2-aminomethyl)bis(2-pyridylmethyl)amine (DPEA) were synthesized by following published procedures.[39,40] Styrene and cyclohexene were passed through a column of activated alumna prior to use in catalytic oxidation experiments. All solvents were purified and/or dried by standard techniques and distilled prior to use.

Synthesis Safety Note. Perchlorate salts should be handled with caution. Although no explosion was encountered in this work, metal perchlorates could detonate upon heating.

Synthesis of Compounds. *N*,*N*-bis(2-pyridylmethyl)amine-*N*-ethyl-2-pyridine-2-carboxamide ($PaPy_3H$). A solution of 1.44 g (5.93 mmol) of DPEA in 10 mL of tetrahydrofuran (THF) was added slowly to a solution of 0.84 g (5.93 mmol) of 2-picolinic acid chloride (obtained by refluxing 2-picolinic acid in thionyl chloride) and excess triethylamine (1.5 g) in 20 mL of THF at 0 °C. The resulting solution was allowed to stir at 0 °C for 20 min. followed by gentle heating to 50 °C for 30 min. The solution was then cooled to 0 °C and filtered to remove $Et_3N{\cdot}HCl$. Removal of the THF in vacuo afforded crude $PaPy_3H$ as a viscous oil. The oil was placed in 30 mL of H_2O and the solution was made basic by addition of NaOH. $PaPy_3H$ was then extracted from the

(28) Zheng, H.; Zang, Y.; Dong, Y.; Young, V. G., Jr.; Que, L., Jr. *J. Am. Chem. Soc*. **1999**, *121*, 2226.
(29) Marlin, D. S.; Olmstead, M. M.; Mascharak, P. K. *Inorg. Chem*. **1999**, *38*, 3258.
(30) Tyler, L.; Noveron, J. C.; Olmstead, M. M.; Mascharak, P. K. *Inorg. Chem*. **1999**, *38*, 616.
(31) Marlin, D. S.; Mascharak, P. K. *Chem. Soc. Rev*. **2000**, *29*, 69.
(32) Brown, S. J.; Olmstead, M. M.; Mascharak, P. K. *Inorg. Chem*. **1990**, *29*, 3229.
(33) Tao, X.; Stephan, D. W.; Mascharak, P. K. *Inorg. Chem.* **1987**, *26*, 754.
(34) Ray, M.; Ghosh, D.; Shirin, Z.; Mukherjee, R. *Inorg. Chem*. **1997**, *36*, 3568.
(35) Patra, A. K.; Mukherjee, R. *Polyhedron* **1999**, *18*, 1317.
(36) Ménage, S.; Wilkinson, E. C.; Que, L., Jr. Fontecave, M. *Angew. Chem., Int. Ed. Engl*. **1995**, *34*, 203.
(37) Kim, J.; Larka, E.; Wilkinson, E. C.; Que, L., Jr. *Angew. Chem., Int. Ed. Engl*. **1995**, *34*, 2048.
(38) Rabion, A.; Chen, S.; Wang, J.; Buchanan, R. M.; Series, J.-L.; Fish, R. H. *J. Am. Chem. Soc*. **1995**, *117*, 12356.
(39) Hodgkinson, J.; Jordan, R. B. *J. Am. Chem. Soc*. **1973**, *95*, 763.
(40) Matouzenko, G. S.; Bousseksou, A.; Lecocq, S.; van Koningsbruggen, P. J.; Perrin, M.; Kahn, O.; Collet, A. *Inorg. Chem*. **1997**, *36*, 2975.

Table 1. Summary of Crystal Data and Intensity Collection and Structure Refinement Parameters for $[Fe(PaPy_3)CH_3CN](ClO_4)_2 \cdot CH_3CN \cdot 0.25H_2O$ ($1 \cdot CH_3CN \cdot 0.25H_2O$), $[Fe(PaPy_3)Cl]ClO_4 \cdot 2CH_3CN$ ($2 \cdot 2CH_3CN$), and $[Fe(PaPy_3)CN]ClO_4 \cdot THF$ ($3 \cdot THF$)

	1	**2**	**3**
empirical formula	$C_{24}H_{26.5}N_7O_5Cl_2Fe$	$C_{24}H_{26}N_7O_5Cl_2Fe$	$C_{25}H_{28}N_6O_6ClFe$
fw	687.77	619.27	559.83
cryst size, mm^3	$0.22 \times 0.20 \times 0.05$	$0.29 \times 0.17 \times 0.03$	$0.45 \times 0.22 \times 0.12$
cryst color, habit	purple plate	red plate	purple block
T, K	90(2)	90(2)	90(2)
cryst system	monoclinic	monoclinic	monoclinic
space group	$P2_1/c$	$P2_1$	$P2_1/c$
a, Å	11.3932	8.4292(3)	8.4996
b, Å	22.2910	14.1990(5)	20.4898
c, Å	12.4489	11.3770(4)	14.7179
α, deg	90	90	90
β, deg	113.48	98.8510	101.2340
γ, deg	90	90	90
vol, $Å^3$	2899.7	1345.45(8)	2514.1
Z	4	2	4
density (calcd), g cm^{-3}	1.575	1.529	1.585
abs coeff, mm^{-1}	0.769	0.808	0.761
GOF[a] on F^2	0.893	0.996	0.954
R_1,[b] %	5.33	3.28	4.97
R_{w2},[c] %	10.78	7.30	10.40

[a] GOF $= [\sum[w(F_o^2 - F_c^2)^2]/(M - N)]^{1/2}$ (M = number of reflections, N = number of parameters refined). [b] $R_1 = \sum||F_o| - |F_c||/\sum|F_o|$. [c] $R_{w2} = [\sum[w(F_o^2 - F_c^2)^2]/\sum[w(F_o^2)^2]]^{1/2}$.

aqueous layer by 3 × 10 mL portions of methylene chloride (CH_2Cl_2). The CH_2Cl_2 layers were collected and dried over $CaSO_4$ and finally removed to yield pure $PaPy_3H$ as a light yellow oil (70% yield). ^1H NMR (303 K, $CDCl_3$, 250 MHz): δ (ppm from TMS), 2.88 (t 2H) 3.61 (q 2H), 3.97 (s 4H), 7.14 (m 2H), 7.32 (m 1H), 7.58 (d 4H), 7.86 (t 1H), 8.20 (d 1H), 8.55 (d 2H), 8.66 (d 1H), 8.72 (s 1H). Selected IR frequency (NaCl plate) $\nu_{co} = 1666$ cm^{-1}.

$[Fe(PaPy_3)(CH_3CN)](ClO_4)_2 \cdot CH_3CN \cdot 0.25H_2O$ ($1 \cdot CH_3CN \cdot 0.25H_2O$). A batch of 0.02 g (0.84 mmol) of NaH was slowly added to a solution of 0.160 g (0.48 mmol) of $PaPy_3H$ dissolved in 12 mL of *N*,*N*′-dimethylformamide (DMF). To this solution of the deprotonated ligand was added dropwise with stirring a solution of 0.347 g (0.48 mmol) of $[Fe(DMF)_6](ClO_4)_3$ in 8 mL of DMF and the resulting red mixture was stirred for 3 h. Next, the solvent was removed and the red oily residue was washed several times with THF. After succesive THF washes, the red oil solidified. The resulting red solid was disolved in 10 mL of acetonitrile (CH_3CN) to afford a dark purple solution. This purple solution afforded dark purple crystals of **1** upon standing at room temperature following addition of 5 mL of diethyl ether. Yield: 30%. Anal. Calcd for $C_{24}H_{26.5}N_7O_{9.25}Cl_2Fe$: C, 41.91; H, 3.88; N, 14.26. Found: C, 41.83; H, 3.79; N, 14.32. Selected IR frequencies (KBr disk, cm^{-1}): 3420 (m), 3086 (w), 2293 (w, ν_{CH3CN}), 1655 (s, ν_{CO}), 1609 (s), 1450 (m), 1356 (m), 1285 (w), 1090 (vs, ν_{ClO4}), 768 (s), 690 (m), 624 (s). Absorption spectrum in CH_3CN, λ_{max} nm (ϵ, $M^{-1}cm^{-1}$): 555(2 800), 350 (2 500).

$[Fe(PaPy_3)(Cl)]ClO_4 \cdot 2CH_3CN$ ($2 \cdot 2CH_3CN$). A batch of 0.033 g (1.38 mmol) of NaH was slowly added to a solution of 0.290 g (0.86 mmol) of $PaPy_3H$ dissolved in 20 mL of DMF. To this solution of the deprotonated ligand was added 0.050 g (0.86 mmol) of NaCl(s) followed by dropwise addition of 0.683 g (0.86 mmol) of $[Fe(DMF)_6](ClO_4)_3$ in 10 mL of DMF. The resulting red solution was allowed to stir for 1 h and then warmed to 45 °C for 30 min. Removal of DMF afforded a red oil which was washed with succesive portions of THF. The resulting red solid was disolved in CH_3CN and filtered to remove any unreacted NaCl. Red crystals of **2** were obtained from crystallization from CH_3CN/diethyl ether solution at −28 °C. Yield: 40%. Anal. Calcd for $C_{24}H_{26}N_7O_5Cl_2Fe$: C, 46.55; H, 4.23; N, 15.83. Found: C, 46.61; H, 4.27; N, 15.72. Selected IR frequencies (KBr disk, cm^{-1}): 3420 (s), 3090 (w), 1634 (s, ν_{CO}), 1605 (s), 1450 (m), 1367 (m), 1283 (w), 1086 (vs, ν_{ClO4}), 880 (w), 766 (s), 691 (m), 623 (s). Absorption spectrum in CH_3CN, λ_{max} nm (ϵ, $M^{-1}cm^{-1}$): 510 (3 200), 365 (3 900).

Alternatively, **2** was obtained by the addition of Et_4NCl at room temperature to solution of **1** in CH_3CN.

$[Fe(PaPy_3)(CN)]ClO_4 \cdot THF$ ($3 \cdot THF$). A batch of 0.017 g (0.71 mmol) of NaH was slowly added to a solution of 0.145 g (0.44 mmol) of $PaPy_3H$ dissolved in 12 mL of DMF. To this solution of the deprotonated ligand was added a batch of 0.022 g (0.45 mmol) of NaCN(s) followed by dropwise addition of 0.318 g (0.44 mmol) of $[Fe(DMF)_6](ClO_4)_3$ in 8 mL of DMF. The purple solution was stirred at room temperature for 4 h. Removal of the DMF afforded a dark red-purple oil which was washed with THF. The resulting solid was disolved in CH_3CN and filtered. Dark red-purple crystals were obtained by recrystallization from CH_3CN/THF solution at −28 °C. Yield: 45%. Anal. Calcd for $C_{25}H_{28}N_6O_6ClFe$: C, 50.06; H, 4.71; N, 14.01. Found: C, 50.16; H, 4.63; N, 14.13. Selected IR frequencies (KBr disk, cm^{-1}): 3420 (s), 2131 (w, ν_{CN}), 1635 (s, ν_{CO}), 1605 (s), 1473 (m), 1447 (m), 1373 (m), 1287 (w), 1089 (vs, ν_{ClO4}), 880 (w), 762 (m), 689 (m), 627 (s). Absorption spectrum in CH_3CN, λ_{max} nm (ϵ, $M^{-1}cm^{-1}$): 533 (1 800), 340 (4 000), 310 (sh, 4900).

Complex **3** was also obtained by the addition of either NaCN or $(Et_4N)(CN)$ at room temperature to solutions of **1** in CH_3CN.

$[Fe(PaPy_3)(N_3)]ClO_4$ (4). This complex was obtained by the addition of NaN_3 or $(Et_4N)(N_3)$ to a solution of **1** in CH_3CN. The addition of either azide salt in slight excess to **1** in CH_3CN resulted in a color change from purple to red. The solution was stirred for 1 h and then filtered to remove any unreacted salt. Red crystals of **4** were obtained from CH_3CN/diethyl ether solution at −28 °C. Yield: 38%. Anal. Calcd for $C_{20}H_{20}N_8O_5ClFe$: C, 44.18; H, 3.71; N, 20.61. Found: C, 44.20; H, 3.67; N, 20.70. Selected IR frequencies (KBr disk, cm^{-1}): 3423 (s), 2043 (w, ν_{N3}), 1637 (s, ν_{CO}), 1604 (s), 1439 (m), 1365 (m), 1284 (w), 1086 (vs, ν_{ClO4}), 767 (m), 690 (m), 624 (s). Absorption spectrum in CH_3CN, λ_{max} nm (ϵ, $M^{-1}cm^{-1}$): 527 (3 900), 360 (3 500).

X-ray Data Collection and Structure Solution and Refinement. Diffraction experiments were performed on a Bruker SMART 1000 diffractometer and data were collected at 90 K. The structures were solved by the use of SHELXS-97 package and the data were corrected for absorption effects. The intensities of two standard reflections showed no significant decay during the course of data collection. Machine parameters, crystal data, and data collection parameters are summarized in Table 1 while selected bond distances and angles are listed in Table 2.

Oxidation Reactions with 1. All reactions were performed in loosely capped vials (atmospheric pressure) and in each case evolution of oxygen gas was apparent. No attempt was made to exclude dioxygen from the reaction mixtures. In a typical reaction, 150 equiv of H_2O_2 (30%) was added to an acetonitrile solution of 15.0 μmol of **1** in the presence of 200 equiv of substrate at room temperature. After 5 min of reaction, an aliquot of the reaction mixture was taken out and filtered through a 0.45 mm Acrodisc Nylon filter. A known amount of internal standard (cyclooctane) was added to the filtrate and the mixture was

Table 2. Selected Bond Lengths (Å) and Angles (deg) for $[Fe(PaPy_3)CH_3CN](ClO_4)_2 \cdot CH_3CN \cdot 0.25H_2O$ (**1**·CH_3CN·$0.25H_2O$), $[Fe(PaPy_3)Cl]ClO_4 \cdot 2CH_3CN$ (**2**·$2CH_3CN$), and $[Fe(PaPy_3)CN]ClO_4 \cdot THF$ (**3**·THF)

	complex **1**	complex **2**	complex **3**
	Bond Lengths (Å)		
Fe−N(1)	1.976(3)	1.9801(18)	1.981(2)
Fe−N(2)	1.826(3)	1.8559(17)	1.858(2)
Fe−N(3)	1.972(3)	1.9880(17)	1.988(2)
Fe−N(4)	1.968(3)	1.9885(16)	1.978(2)
Fe−N(5)	1.968(3)	1.9902(17)	1.994(2)
Fe−N(6)	1.982(3)		
Fe−Cl		2.2833(5)	
Fe−CN			1.974(3)
O(1)−C(6)	1.237(4)	1.233(3)	1.238(3)
N(2)−C(6)	1.349(4)	1.340(3)	1.342(3)
N(3)−C(15)	1.486(5)	1.494(3)	1.495(3)
	Bond Angles (deg)		
N(1)−Fe−N(2)	82.92(13)	82.76(7)	82.71(9)
N(1)−Fe−N(3)	168.88(13)	169.05(7)	167.74(9)
N(1)−Fe−N(4)	96.56(13)	97.05(7)	97.58(8)
N(1)−Fe−N(5)	96.99(12)	97.06(7)	96.29(8)
N(1)−Fe−N(6)	96.31(13)		
N(1)−Fe−Cl		94.41(5)	
N(1)−Fe−CN			98.76(9)
N(2)−Fe−N(3)	86.13(13)	86.35(7)	85.25(9)
N(2)−Fe−N(4)	96.85(13)	87.90(7)	89.53(8)
N(2)−Fe−N(5)	88.95(12)	93.01(7)	95.01(8)
N(2)−Fe−N(6)	176.80(12)		
N(2)−Fe−Cl		177.10(6)	
N(2)−Fe−CN			175.09(10)
N(3)−Fe−N(4)	82.80(13)	83.63(7)	84.57(8)
N(3)−Fe−N(5)	84.70(12)	82.36(7)	82.45(8)
N(3)−Fe−N(6)	94.73(12)		
N(3)−Fe−Cl		96.49(5)	
N(3)−Fe−CN			98.76(9)
N(4)−Fe−N(5)	165.82(12)	165.87(7)	165.84(8)
N(4)−Fe−N(6)	86.32(12)		
N(4)−Fe−Cl		91.81(5)	
N(4)−Fe−CN			88.04(9)
N(5)−Fe−N(6)	88.06(12)		
N(5)−Fe−Cl		87.98(5)	
N(5)−Fe−CN			88.34(9)

analyzed by GC (Hewlett-Packard 5890 Series II Plus; flame-ionization detection; Heliflex AT-1701 capillary column (Alltech)). In all cases, addition of H_2O_2 resulted in a change of color from violet to red and a rapid evolution of oxygen. The reaction mixtures were bleached within 5 min. However, when only 15 equiv of H_2O_2 was used, the color persisted for more than 1 h. Under this condition, the rate of O_2 evolution and the rate of oxidation of substrate were both much slower. In case of TBHP, (150 equiv), the color persisted for more than 15 min indicating a longer lifetime of the iron-containing intermediate(s).

Other Physical Measurements. Absorption spectra were recorded on a Perkin-Elmer Lambda 9 spectrophotometer. A Perkin-Elmer 1600 FTIR spectrophotometer was used to monitor the infrared spectra. EPR spectra at X-band frequencies were obtained with a Bruker ESP-300 spectrometer. Electrochemical measurements were performed with standard Princeton Applied Research instrumentation and a Pt-inlay electrode. Halfwave potentials ($E_{1/2}$) were measured vs aqueous saturated calomel electrode (SCE).

Results and Discussion

In recent years, the chemistry of iron(III) complexes with ligated carboxamido nitrogens has been explored to establish the intrinsic properties of iron(III) centers in nitrile hydratase and nitrogenase.[31] As part of this pursuit, several complexes with coordinated carboxamido nitrogens have been synthesized and studied in detail. A recent review on such complexes points out that all reported complexes contain 2−4 carboxamido nitrogens as donors.[31] Complexes **1**−**3** comprise the first set of

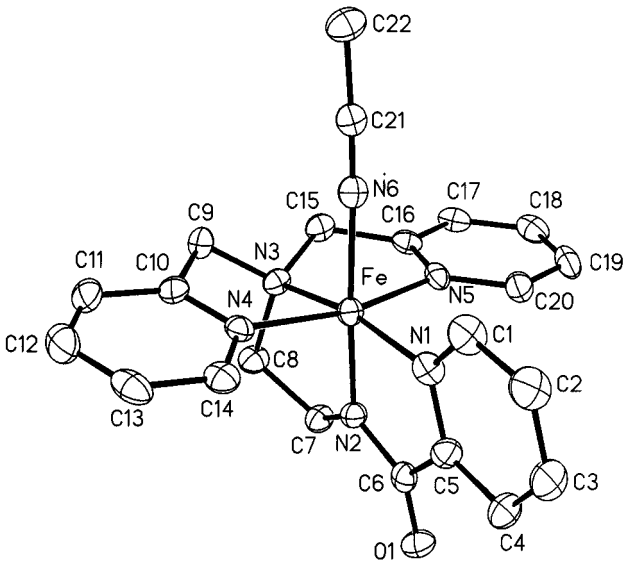

Figure 2. Thermal ellipsoid (probability level 50%) plot of $[Fe(PaPy_3)(CH_3CN)]^{2+}$ (cation of **1**) with the atom-labeling scheme. H atoms are omitted for the sake of clarity.

structurally characterized six coordinate iron(III) species that contain a *single* carboxamido nitrogen in the first coordination sphere. Out of this set, $[Fe(PaPy_3)(CH_3CN)]^{2+}$ is particularly interesting since the iron(III) center in this complex is ligated by an easily exchangeable solvent (CH_3CN) molecule at the sixth site. Although ligands such as N4Py and Py5[21,22] give rise to iron(II) complexes[10,13,21] of the type $[LFe(CH_3CN)]^{2+}$, deprotonated $PaPy_3^-$ readily affords the iron(III) complexes **1**−**3**. This altered reactivity arises from the extra stability carboxamido nitrogens provide to iron(III), a fact noted by us previously.[29,31] The extra stability also allowed us to synthesize the carboxamido complexes directly from iron(III) sources without going through oxidation of an isolated iron(II) complex.[41] Facile exchange of the coordinated acetonitrile ligand with various anionic ligands affords $[Fe(PaPy_3)(Cl)]^+$ (**2**), $[Fe(PaPy_3)(CN)]^+$ (**3**), and $[Fe(PaPy_3)(N_3)]^+$ (**4**) without any complication. The clean ligand exchange reactions also prompted us to investigate the possibility of generating [LFe(OOR)] species via reaction of **1** with H_2O_2 and TBHP. Here we report that one can synthesize [LFe(OOR)] (R = ^{t}Bu, H) species by a simple ligand exchange reaction between **1** and TBHP or H_2O_2, respectively. The resulting $[LFe(OOR)]^+$ species are highly reactive species and can be used for various oxidation reactions.

The structures of the cations of **1**−**3** are shown in Figures 2−4, respectively, and selected bond distances and angles are listed in Table 2. The geometry around the iron(III) center in all three species is distorted octahedral. In all three complexes, the $PaPy_3^-$ ligand is bound to iron in a pentadentate square pyramidal fashion with three pyridine nitrogens, one tertiary amine nitrogen, and one carboxamido nitrogen as donors. The carboxamido nitrogen is trans to the exchangeable ligand at the sixth site. In **1** (Figure 2), an acetonitrile molecule occupies the sixth site on iron while in **2** (Figure 3) and **3** (Figure 4) octahedral coordination is completed by a chloride ion and a cyanide ion, respectively.

In complex **1**, the Fe(III)−N_{amido} bond length is exceptionally short (1.826(3) Å). The corresponding bonds in **2** and **3** are also quite short (1.8559(17), 1.858(2) Å respectively) compared to other Fe(III)−N_{amido} bonds reported so far (range 1.88−2.23

(41) Noveron, J. C.; Herradora, R.; Olmstead, M. M.; Mascharak, P. K. *Inorg. Chim. Acta* **1999**, *285*, 269.

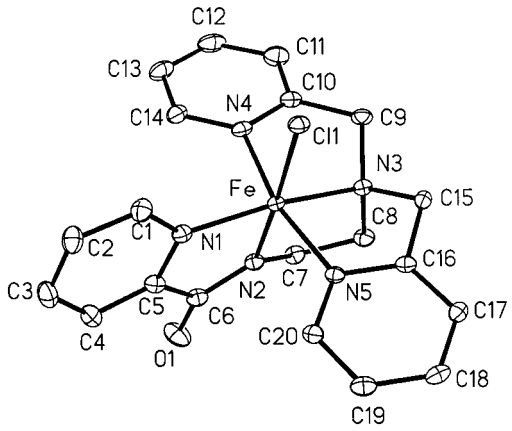

Figure 3. Thermal ellipsoid (probability level 50%) plot of $[Fe(PaPy_3)(Cl)]^+$ (cation of **2**) with the atom-labeling scheme. H atoms are omitted for the sake of clarity.

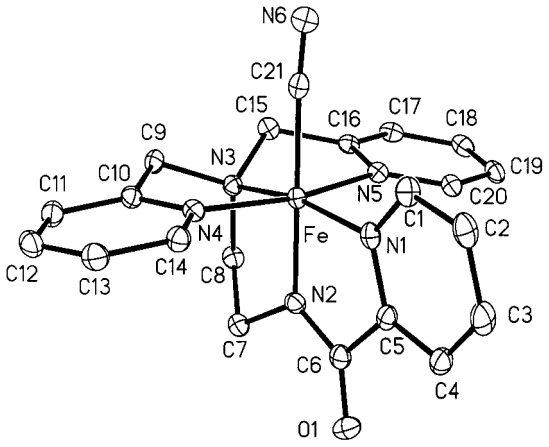

Figure 4. Thermal ellipsoid (probability level 50%) plot of $[Fe(PaPy_3)(CN)]^+$ (cation of **3**) with the atom-labeling scheme. H atoms are omitted for the sake of clarity.

Å).[31] Examples of complexes with short Fe(III)−N_{amido} bonds include $[Fe(bpc)(1\text{-}MeIm)_2]^+$ (1.886(4) Å, bpc = 4,5-dichloro-1,2-bis(pyridine-2-carboxamido)-benzene)[42] and the macrocyclic species $[Fe(H_2O)(L_3)]^-$ (1.867(3) Å, L_3 = 13,14-dichloro-6,6-diethyl-2,5,710(6*H*,11*H*)-tetraoxo-3,3,9,9-tetramethyl-1*H*-1,4,8,11-benzotetraazacyclotridecine).[43] Both the low spin nature of the iron(III) center and the overall positive charge of the complex are presumably responsible for the very short Fe(III)−N_{amido} bond in **1**. The slight lengthening of the Fe(III)−N_{amido} bond in **2** and **3** results from the binding of anionic ligands (Cl^- and CN^- respectively).

In complex **1**, the Fe(III)−N_{CH3CN} bond is 1.982(3) Å long. Since no other Fe(III)−N_{CH3CN} bond length for this type of complexes is reported in the literature, we here compare complex **1** with Fe(II) complexes with similar ligand frameworks.[44] The Fe(III)−N_{CH3CN} bond of complex **1** is longer than that noted in $[Fe(TPA)(CH_3CN)_2](ClO_4)_2$. (1.93(1) and 1.92(1) Å),[15] $[Fe(N4Py)(CH_3CN)](ClO_4)_2$ (1.915(3) Å),[13] and $[(Py5)Fe(CH_3CN)](ClO_4)_2$ (1.952(8) Å).[21] The fact that the Fe(III)−N_{CH3CN} distance in **1** is longer than the Fe(II)−N_{CH3CN} distances in analogous complexes is intriguing. The observed elongation of the Fe(III)−N_{CH3CN} bond in **1** cannot arise from steric repulsions and must result from electronic effects induced by the carboxamido nitrogen trans to the ligated acetonitrile.

The average Fe(III)−N_{py} (py = pyridine) distance of 1.968 (3) Å in complex **1** is comparable to that observed with other low spin mononuclear Fe(III) complexes such as $[(5\text{-}Me_3\text{-}TPA)Fe(acac)]^{2+}$ (1.953(3) Å).[16] However, it is interesting to note that both the Fe(III)−N_{py} and Fe(III)−N_{amine} (1.972 (3) Å) bonds of **1** are considerably shorter than the Fe(III)−N_{py} and Fe(III)−N_{amine} bonds in dinuclear high spin Fe(III) complexes of TPA like $[(TPA)(Cl)FeO(Cl)(TPA)](ClO_4)_2$ (2.148(12) and 2.227(6) Å respectively).[23]

In complex **2**, the Fe(III)−Cl bond is 2.2833 (5) Å long. This distance is slightly shorter than Fe(III)−Cl distances in spin-coupled oxo-bridged Fe(III) dimers of TPA (2.319 (2) Å)[23] and related ligands (range 2.34−2.33 Å).[26] The Fe(III)−CN distance in **3** (1.974 (3) Å) is close to that noted with $K_3[Fe(CN)_6]$ (1.95 (2) Å)[45] and $K[Fe(TPP)(CN)_2]$ (1.975 (2) Å).[46]

Spectroscopic and Redox Properties. Coordination of the carboxamido nitrogen to the iron(III) center is evidenced by the shift of the carbonyl stretch (ν_{CO}) from 1666 cm^{-1} in free $PaPy_3H$ to 1655 cm^{-1} in complex **1**.[31] The presence of Cl^- and CN^- shifts ν_{CO} further to 1634 cm^{-1} (complex **2**) and 1635 cm^{-1} (complex **3**), respectively. This red shift of ν_{CO} results from an increase of negative charge at the Fe(III) center in the latter two complexes. Complex **3** exhibits ν_{CN} at 2130 cm^{-1}. All three complexes dissolve in solvents such as DMF, acetonitrile, and methanol to afford solutions with characteristic colors. For example, in acetonitrile, **1** and **3** give rise to intense purple and burgundy solutions, respectively, while **2** and **4** afford deep red solutions. The colors arise from strong ligand-to-metal charge transfer (LMCT) bands which are similar to absorption bands of other low spin iron(III) complexes with carboxamido nitrogen ligation.[29,32,33] Solutions of both **1** and **2** in water exhibit the same electronic spectrum (λ_{max} = 500 nm), a fact that suggests the formation of $[Fe(PaPy_3)(H_2O)]^{2+}$ by displacement of acetonitrile or chloride by a water molecule. It is important to note that aqueous solutions of complexes **1**−**3** are stable for days at room temperature with no indication of complex degradation. Thus, the common notion that the strongly basic carboxamido nitrogens are readily attacked by water appears unlikely in this chemistry. Also formation of oxo- and/or hydroxo-bridged polymeric iron(III) species as hydrolytic decomposition products is not observed with complexes of this type. We have previously discussed this fact in relation to other iron(III) complexes with carboxamido nitrogens as donors.[29,31]

The redox properties of **1**−**4** have been investigated by voltammetric techniques. Complex **1** exhibits a reversible voltammogram in acetonitrile with an $E_{1/2}$ value of 0.21 V vs SCE. In contrast, $[Fe(N4Py)(CH_3CN)](ClO_4)_2$ and $[(Py5)Fe(CH_3CN)](ClO_4)_2$ comprise highly stabilized iron(II) centers and exhibit very high oxidation potentials ($E_{1/2}$ = 1.01 and 1.21 V vs SCE, respectively) in acetonitrile. When one compares the $E_{1/2}$ values of these three iron complexes with the very similar N5 chromophore and one bound acetonitrile, it becomes evident that the presence of *one* carboxamido nitrogen in the first coordination sphere of iron provides about 1 V of stabilization to the +3 oxidation state. Coordination of anions such as Cl^-

(42) Che, C.-M.; Leung, W.-H.; Cheng, H.-Y.; Peng, S.-M. *Inorg. Chim. Acta* **1992**, *196*.
(43) Bartos, M. J.; Kidwell, C.; Kauffmann, K. E.; Gordon-Wylie, S. W.; Collins, T. J.; Clark, G. C.; Münck, E.; Wientraub, S. T. *Angew. Chem., Int. Ed. Engl.* **1995**, *34*, 1216.
(44) In the Fe(III) complex $[T_pPr^i{}_2Fe^{III}(DBC)(CH_3CN)]$ (*Inorg. Chem.* **1998**, *37*, 2614), the CH_3CN molecule is loosely bound due to steric effect ($T_pPr^i{}_2$ = sterically crowded substituted tris(pyrazolyl)borate, DBC = di-^{t}butylcatecholate). The Fe(III)−N_{CH3CN} distance in this complex is 2.326 (5) Å.
(45) Vannerberg, N. G. *Acta Chem. Scand.* **1972**, *26*, 2863.
(46) Scheidt, W. R.; Haller, K. J.; Hatano, K. *J. Am. Chem. Soc*. **1980**, *102*, 3017.

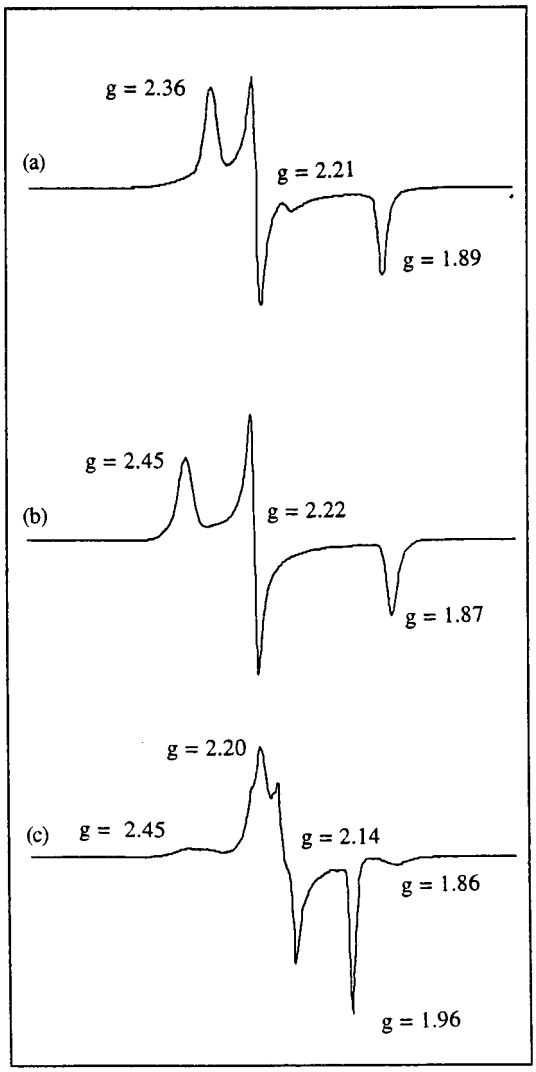

Figure 5. X-band EPR spectra of (a) $[Fe(PaPy_3)(CH_3CN)](ClO_4)_2$ (**1**), (b) $[Fe(PaPy_3)(Cl)](ClO_4)$ (**2**), and $[Fe(PaPy_3)(OOH)]^+$ in DMF/CH_3-CN (70:30) glass (80 K). The g values are indicated. Spectrometer settings: microwave power, 13 mW; microwave frequency, 9.43 GHz; modulation frequency, 100 kHz; modulation amplitude, 2 G.

and CN^- further shift the $E_{1/2}$ value to −0.03 V and −0.01 V (vs SCE) for complexes **2** and **3**, respectively. It thus appears that the addition of a second anionic ligand such as Cl^- or CN^- to the first coordination sphere of **1** provides further stabilization, albeit to a smaller extent, to the +3 oxidation state of iron. With azide (N_3^-) at the sixth site of iron, **4** exhibits its $E_{1/2}$ at −0.14 V (vs SCE in acetonitrile) indicating the highest stabilization of the Fe(III) center among the present complexes **1**−**4**.

The results of susceptibility measurements at room temperature with polycrystalline **1**−**4** indicate that these complexes are all low spin ($\mu = 2.1-2.3\ \mu_B$). The low spin configuration is also supported by the EPR spectra of **1**−**4** in acetonitrile/methanol glass (Figure 5). Addition of water to CH_3CN/DMF solutions of **1** does not bring about a change in the spin state and $[Fe(PaPy_3)(H_2O)]^{2+}$ displays a low spin EPR signal (g = 2.42, 2.21, 1.88).

Interconversions of 1−4. Interconversions of the present complexes **1**−**4** have been followed by spectrophotometry. Conversion of **1** into **2** is readily achieved by the addition of a soluble source of chloride (like Et_4NCl) to a solution of **1** in acetonitrile or DMF (Scheme 1). The overall superior stability of **2** is indicated by the fact that one can convert **1** into **2** just by warming (to 40 °C) a solution of **1** in acetonitrile in the presence of a very slight excess of an insoluble chloride source like NaCl. When **2** is allowed to react with 1 equiv of $AgClO_4$ in acetonitrile at room temperature, the red (λ_{max} = 510 nm) to purple (λ_{max} = 555 nm) color change indicates the displacement of the chloride anion by Ag^+ and the formation of complex **1** (Scheme 1).

Scheme 1

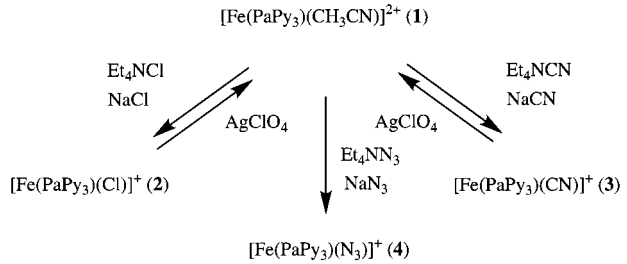

Table 3. EPR Data for Low Spin $[LFe^{III}-OOH]$ Complexes

complex	g_1	g_2	g_3
$[Fe^{III}(PaPy_3)(OOH)]^+$	2.24	2.14	1.96[a]
$[Fe^{III}(N^4Py)(OOH)]^{2+}$	2.17	2.12	1.98[b]
$[Fe^{III}(Py^5)(OOH)]^{2+}$	2.15	2.13	1.98[c]
$[Fe^{III}(tmpy)(OOH)]^{2+}$	2.19	2.12	1.95[d]
$[Fe^{III}(TPA)(S)(OOH)]^{2+}$	2.19	2.15	1.97[e]
$[Fe^{III}(PMA)(OOH)]^+$	2.27	2.18	1.93[f]
$[Fe^{III}(BLM)(OOH)]$	2.26	2.17	1.94[g]

[a] This work. [b] Ref 13. [c] Ref 21. [d] Refs 19 and 20. [e] Ref 15. [f] Ref 8. [g] Sam, J. W.; Tang, X.-J.; Peisach, J. *J. Am. Chem. Soc.* **1994**, *116*, 5250. Burger, R. M.; Peisach, J.; Horwitz, S. B. *J. Biol. Chem.* **1981**, *256*, 11636. For additional discussion see: Solomon, E. I.; Brunold, T. C.; Davis, M. I.; Kemsley, J. N.; Lee, S.-K.; Lehnert, N.; Neese, F.; Skulan, A. J.; Yang, Y.-S.; Zhou, J. *Chem. Rev.* **2000**, *100*, 235. Neese, F.; Zaleski, J. M.; Zaleski, K. L.; Solomon, E. I. *J. Am. Chem. Soc.* **2000**, *122*, 11703.

Removal of the solid AgCl by filtration followed by the addition of diethyl ether affords crystalline **1**. A similar color change is observed when an acetonitrile solution of **3** (λ_{max} = 533 nm) is treated with 1 equiv of $AgClO_4$. Complete displacement of the cyanide ligand is only achieved upon gentle warming of the solution. This is indicated by the development of the purple color of **1** (λ_{max} = 555 nm) upon heating (Scheme 1). As shown in Scheme 1, **3** is readily obtained from **1** upon addition of CN^- to **1** in acetonitrile or DMF. Finally, addition of NaN_3 (or $(Et_4N)(N_3)$) to solution of **1** in acetonitrile or DMF affords **4** (λ_{max} = 527) in high yield.

Formation of $[Fe(PaPy_3)(OOH)]^+$ and Its Reactivity. Addition of H_2O_2 to $[Fe(PaPy_3)(CH_3CN)]^{2+}$ (**1**) in DMF/CH_3-CN at low temperature results in noticeable changes in its EPR spectrum. As shown in Figure 5, the product exhibits a low spin EPR signal much like the [LFe(OOH)] species reported by us and other groups (Table 3). This clearly shows that $[Fe(PaPy_3)(CH_3CN)]^{2+}$ does afford the low spin peroxo-iron(III) species $[Fe(PaPy_3)(OOH)]^+$ by direct ligand exchange in solution. However, much like the other peroxo-iron(III) species, $[Fe(PaPy_3)(OOH)]^+$ is quite reactive and is decomposed within minutes when the reaction mixture is warmed to room temperature. This is evidenced by the loss of the red color along with effervescence. EPR measurements also indicate that $[Fe(PaPy_3)(OO^tBu)]^+$, formed upon addition of TBHP to **1** in DMF/CH_3CN at low temperature, is even more reactive and decomposes at liquid N_2 temperature. We could only detect weak signals for $[Fe(PaPy_3)(OO^tBu)]^+$ at g = 2.21, 2.14, and 1.93 (80 K). The EPR spectrum was invariably dominated by strong

Table 4. Results of Hydrocarbon Oxidations by **1** in Conjuction with H_2O_2, TBHP, and MPPH[b]

catalyst	oxidant	substrate	products (TN[b])
$[Fe(PaPy_3)(CH_3CN)]^{2+}$	H_2O_2 (150 equiv)	cyclohexene	cyclohexene oxide (17) 2-cyclohexen-1-one (3) 2-cyclohexen-1-ol (3)
$[Fe(PaPy_3)(CH_3CN)]^{2+}$	H_2O_2 (20 equiv)	cyclohexene	cyclohexene oxide (3) 2-cyclohexen-1-one (0.7) 2-cyclohexen-1-ol (0.9)
$[Fe(PaPy_3)(CN)]^{+}$	H_2O_2 (150 equiv)	cyclohexene	cyclohexene oxide (trace) 2-cyclohexen-1-one (trace) 2-cyclohexen-1-ol (trace)
$[Fe(PaPy_3)(CH_3CN)]^{2+}$ + 10 equiv $(Et_4N)(CN)$	H_2O_2 (150 equiv)	cyclohexene	cyclohexene oxide (trace) 2-cyclohexen-1-one (trace) 2-cyclohexen-1-ol (trace)
$[Fe(PaPy_3)(CH_3CN)]^{2+}$ + DMS	H_2O_2 (150 equiv)	cyclohexene	cyclohexene oxide (0.5) 2-cyclohexen-1-one (3) 2-cyclohexen-1-ol (3)
$[Fe(PaPy_3)(CH_3CN)]^{2+}$	H_2O_2 (150 equiv)	styrene	styrene oxide (25) benzaldehyde (13)
$[Fe(PaPy_3)(CH_3CN)]^{2+}$	TBHP (150 equiv)	cyclohexene	cyclohexene oxide (trace) 2-cyclohexen-1-one (9) 2-cyclohexen-1-ol (7) mixed peroxide
$[Fe(PaPy_3)(CH_3CN)]^{2+}$	MPPH (150 equiv)	cyclohexene	cyclohexene oxide (0) 2-cyclohexen-1-one (0.5) 2-cyclohexen-1-ol (0.6) benzaldehyde (5)
$[Fe(PaPy_3)(CH_3CN)]^{2+}$	H_2O_2 (150 equiv)	cyclohexane	cyclohexanol (9) cyclohexanone (9)
$[Fe(PaPy_3)(CN)]^{+}$	H_2O_2 (150 equiv)	cyclohexane	cyclohexanol (trace) cyclohexanone (trace)
$[Fe(PaPy_3)(CH_3CN)]^{2+}$	TBHP (150 equiv)	cyclohexane	cyclohexanol (5) cyclohexanone (7) mixed peroxide
$[Fe(PaPy_3)(CH_3CN)]^{2+}$	MPPH (150 equiv)	cyclohexane	cyclohexanol (trace) cyclohexanone (trace) benzaldehyde (5)

[a] See Experimental Section for complete description of reaction conditions. [b] TN = turnover number.

signals around $g = 2.01$ presumably due to $^tBuO^\bullet$ and/or $^tBuOO^\bullet$ radical(s) in the sample tube.

Detection of a reactive peroxo-iron(III) species in solution raised the possibility of employing mixtures of **1** and H_2O_2 in promoting oxidation of hydrocarbons under mild conditions. We have therefore investigated the reactivity of $[Fe(PaPy_3)(OOH)]^+$ toward selected hydrocarbons. The results of the oxidation reactions with $[Fe(PaPy_3)(OOH)]^+$ are shown in Table 4 where the turnover numbers (TN) are calculated as moles of products per mole of **1** as the catalyst.

In recent years, work from the research groups of Que and Ingold has indicated that although low spin peroxo-iron(III) species could be identified in reaction mixtures of iron complexes and alkyl hydroperoxides, oxidation of C−H bonds by such mixtures is promoted by incipient O-based radicals.[47−49] In some cases, epoxidation of hydrocarbon substrates with double bonds has also been observed with specific iron complexes and H_2O_2.[15,50,51] This latter reactivity along with the recent findings of Que and co-workers in the area of stereospecific hydroxylation[15,52−54] suggests that a different, possibly metal-based, oxidant could be present in the reaction mixtures when H_2O_2 is employed. With these results in mind, we selected cyclohexene as our first substrate. Oxidation of cyclohexene with **1** and H_2O_2 in acetonitrile affords cyclohexene oxide (TN = 17) as the primary product. In addition, lesser amounts of the allylic oxidation products 2-cyclohexen-1-one and 2-cyclohexen-1-ol (1:1, TN = 3) are also obtained. That the iron complex **1** is essential for this reaction is indicated by the complete shut down of the oxidation when the reaction mixture contains 10 equiv of CN^-. As discussed in previous sections, **1** reacts with CN^- in acetonitrile to form **3**, a complex with no binding site. It is thus clear that initial reaction of **1** with H_2O_2 to form the iron(III)-peroxo intermediate is essential for the initiation of the oxidation reaction. The formation of significant amount of cyclohexene oxide by **1**/H_2O_2 within 5 min is quite notable. In this regard, the present system resembles the $[Fe(cyclam)]^{2+}/H_2O_2$ system of Nam et al. [50,51] and is distinct from the $[Fe(N4Py)(CH_3CN)]^{2+}/H_2O_2$ system reported recently Feringa and co-workers.[13,53,55]

The presence of the allylic oxidation products in 1:1 ratio indicates that a radical-induced autoxidation reaction occurs in parallel in the present system. This is further proved by the fact that use of TBHP in place of H_2O_2 affords only the allylic

(47) MacFaul, P. A.; Arends, I. W. C. E.; Ingold, K. U.; Wayner, D. D. M. *J. Chem. Soc., Perkin Trans. 2* **1997**, 135.
(48) MacFaul, P. A.; Ingold, K. U.; Wayner, D. D. M.; Que, L., Jr. *J. Am. Chem. Soc.* **1997**, *119*, 10594.
(49) Kim, J.; Harrison, R. G.; Kim, C.; Que, L., Jr. *J. Am. Chem. Soc*. **1996**, *118*, 4373.
(50) Nam, W.; Ho, R.; Valentine, J. S. *J. Am. Chem. Soc*. **1991**, *113*, 7052.
(51) Valentine, J. S.; Nam, W.; Ho, R. Y. N. In *The Activation of Dioxygen and Homogeneous Catalytic Oxidation*; Barton, D. H. R., Martell, A. E., Sawyer, D. T., Eds.; Plenum Press: New York, 1993; p. 183.
(52) Chen, K.; Que, L., Jr. *Angew. Chem., Int. Ed. Engl*. **1999**, *38*, 2227.
(53) Roelfes, G.; Lubben, M.; Hage, R.; Que, L., Jr.; Feringa, B. L. *Chem. Eur. J*. **2000**, *6*, 2152.
(54) Chen, K.; Que, L., Jr. *Chem. Commun*. **1999**, 1375.
(55) It is interesting to note that although the $[Fe(N4Py)(CH_3CN)]^{2+}/H_2O_2$ system does not afford a significant amount of cyclohexene oxide with cyclohexene as the substrate, it oxidizes benzene to phenol (TN = 17) in acetonitrile medium. Quite in contrast, the **1**/H_2O_2 system affords significant amounts of cyclohexene oxide and also oxidizes benezene to phenol (TN = 5). Taken together, these results indicate that the $HO^\bullet$ radical most possibly is *not* the species responsible for epoxidation of cyclohexene by **1**/H_2O_2.

oxidation products (1:1 ratio) in similar yields (Table 4). Since O-centered radicals induce allylic oxidation and not epoxidation of cyclohexene,[56] it appears that another oxidizing species is present in the reaction mixture containing **1**, H_2O_2, and cyclohexene. It is tempting to assign this oxidizing species as metal-centered although we do not have any spectroscopic evidence in favor of such a claim. However, it is noteworthy that when the oxidation of cyclohexene is performed with **1**/H_2O_2 in the presence of 90 equiv of dimethyl sulfide, the epoxidation pathway is shut off and only the allylic oxidation products are obtained (Table 4) in addition to a significant amount of dimethyl sulfoxide (TN = 24). Again, this reaction indicates the presence of an oxidant in the reaction mixture that specifically promotes epoxidation of cyclohexene and is inhibited by dimethyl sulfide. In a recent paper, Fontecave and co-workers have reported enantioselective sulfoxidation by the use of an Fe(III) complex and H_2O_2.[57] These researchers have argued on behalf of a metal-centered oxidant as the species responsible for the conversion of sulfide to sulfoxide. Marnett and co-workers have also suggested that sulfoxidation is an evidence for hypervalent iron-oxo intermediates[58] while Ingold and co-workers believe that O-centered radicals are responsible for such conversion.[47,48] Clearly, more work is required to identify the epoxidation agent that is derived from the iron(III)-peroxo species formed initially in the reaction of **1** with H_2O_2.

Complex **1** is also capable of oxidation of cyclohexane with peroxides. As shown in Table 4, reaction of **1**/ROOH (R = ^{t}Bu, H) with cyclohexane in acetonitrile affords moderate yields (TN = 5−9) of cyclohexanol and cyclohexanone in 1:1 ratio within 5 min. The 1:1 cyclohexanol/-one ratio strongly suggests that the oxidation of cyclohexane is carried out by O-centered radicals in such reaction mixtures.[9,47−49] This is further supported by the fact that when the mechanistic probe 2-methyl-1-phenylprop-2-yl hydroperoxide (MPPH)[47] is used as the peroxide, no oxidation of cyclohexane was noted (Table 4). It is thus evident that complex **1** is capable of oxidizing cyclohexane in conjunction with both TBHP and H_2O_2 via the radical pathway and with comparable efficiency. This is in contrast to the case with cyclohexene where **1**/H_2O_2 affords predominantly cyclohexene oxide and **1**/TBHP yields only the allylic oxidation products.

Whether combination of iron(III) complexes (like **1**) and H_2O_2 has unique oxidation capability or not is an open question at this time. We believe that identification of the unique oxidizing intermediate(s) with H_2O_2 could only be possible with measurements on stable iron(III)-peroxo species which in turn could be obtained from properly designed iron(III) complexes. The present work shows that the iron complex of $PaPy_3H$ exhibits very different reactivity compared to other N5-ligands such as N4Py and Py5. However, **1** does not afford an iron(III)-peroxo species stable enough for isolation. Present research in this laboratory is therefore being directed toward syntheses of iron complexes of other designed ligands.

Summary and Conclusions

The following are the summary and conclusions of this work: (a) The iron(III) complexes of the new pentacoordinate peptide ligand $PaPy_3H$ namely $[Fe(PaPy_3)(CH_3CN)](ClO_4)_2$ (**1**), $[Fe(PaPy_3)(Cl)]ClO_4$ (**2**) and $[Fe(PaPy_3)(CN)]ClO_4$ (**3**) have been isolated and structurally characterized. This is the first set of monomeric iron(III) complexes with one carboxamido nitrogen in the coordination sphere. (b) The anionic carboxamido nitrogen in complex **1** provides significant stability to the +3 oxidation state of iron. In acetonitrile, the $E_{1/2}$ value of **1** is 0.21 V (vs SCE) while similar complexes with N5 chromophore (but no carboxamide) like $[Fe(N4Py)(CH_3CN)](ClO_4)_2$ and $[(Py5)Fe(CH_3CN)](ClO_4)_2$ exhibit $E_{1/2}$ values around 1 V (vs SCE). (c) Reactions of $[Fe(PaPy_3)(CH_3CN)]^{2+}$ with H_2O_2 in acetonitrile at low temperature affords $[Fe(PaPy_3)(OOH)]^+$ via simple ligand exchange. This low spin iron(III)-peroxo species is reactive and promotes a significant extent of the epoxidation of cyclohexene at room temperature within minutes. The fact that complex **3** is not capable of any oxidation in the presence of H_2O_2 indicates that formation of $[Fe(PaPy_3)(OOH)]^+$ is a required step in the overall process of oxidation. (d) Analysis of the oxidized products of cyclohexene indicates that while the allylic oxidation is carried out by O-centered radicals, epoxidation is most possibly carried out by a different oxidant produced in the reaction mixture from the initial iron(III)-peroxo intermediate $[Fe(PaPy_3)(OOH)]^+$. (e) With TBHP, **1** initiates oxidation of both cyclohexene and cyclohexane via a radical pathway.

Acknowledgment. Financial support from NSF (CHE-9818492) and NIH (GM 61636) is gratefully acknowledged. The Bruker SMART 1000 diffractometer was funded in part by an NSF Instrumentation Grant CHE-9808259.

Supporting Information Available: X-ray crystallographic files, in CIF format, for the structure determination of **1**−**3**. This material is available free of charge via the Internet at http://pubs.acs.org.

IC001127S

(56) Sheldon, R. A.; Kochi, J. K. In *Metal-Catalyzed Oxidations of Organic Compounds*; Academic Press: New York, 1981; p 26.
(57) Duboc-Toia, C.; Menage, S.; Ho, R. Y. N.; Que, L., Jr.; Lambeaux, C.; Fontecave, M. *Inorg. Chem*. **1999**, *38*, 1261.
(58) Labeque, R.; Marnett, L. R. *J. Am. Chem. Soc*. **1989**, *111*, 6621.